Journal of Materials Chemistry

Cite this: *J. Mater. Chem.*, 2011, **21**, 13015

www.rsc.org/materials

PAPER

Simultaneous determination of paracetamol and neurotransmitters in biological fluids using a carbon paste sensor modified with gold nanoparticles

Nada F. Atta,* Ahmed Galal,* Fekria M. Abu-Attia and Shereen M. Azab

Received 23rd April 2011, Accepted 7th June 2011
DOI: 10.1039/c1jm11795e

A promising electrochemical sensor was developed by electrodeposition of gold nanoparticles on a carbon paste (CP) electrode. This sensor electrode (CPE–Au_{nano}) was used to determine paracetamol (ACOP) and some neurotransmitters, such as dopamine (DA), epinephrine (EP), norepinephrine (NP), levodopa (L-DOPA) and serotonin (5-HT). Cyclic and differential pulse voltammetry studies indicated that the oxidation of paracetamol at the electrode surface proceeded through a two electron reversible step and was fundamentally controlled by adsorption. Further modification of the sensor by mixing the CPE–Au_{nano} with Nafion® showed good sensitivity and effectively resolved the overlapping anodic peaks of these neurotransmitters (NTs) with ACOP. Also, the interfering effect of physiologically common interferences, namely ascorbic acid (AA) and uric acid (UA), on the current response of paracetamol has been studied. Nafion® proved to increase the sensitivity of the current signal of the sensor for the oxidation of the compounds studied. Paracetamol gave a well defined oxidation peak at 430 mV in pH 7.4, which was used to quantitate the drug in the two ranges of 50 nM–50 μM and 90–270 μM with a detection limit of 7.7 nM and 28 nM, respectively. The procedure was successfully validated for the assay of paracetamol in pharmaceutical formulations. The applicability of the developed method to determine the drug in human urine samples is also illustrated.

1. Introduction

Neurotransmitters (NTs) are endogenous chemicals that relay, amplify, and modulate signals between a neuron and another cell; they are widely distributed in the central neural system, brain tissues and body fluids of mammals. The monitoring of NTs is an essential tool in elucidating normal and pathological neural system functions.[1] Trace level measurements in the brain are especially important in studying the role of NTs in neurophysiology, behavioral effects, pathology, disease diagnosis and control since their changes have been associated with various diseases and disorders, such as Parkinson's disease,[2] Alzheimer's disease,[3] Down's syndrome, Huntington's disease,[4] schizophrenia, epilepsy and cocaine addiction.[5]

Dopamine (DA) exists in the human body and can be supplied as a medication. Epinephrine (EP) is biosynthesized in the adrenal medulla and is widely used for the treatment of neural disorders.[6] Norepinephrine (NE) level affects several diseases, such as neuroblastoma, ganglioneuroblastoma, ganglioneuroma, paraganglioma, diabetes mellitus ketoacidosis and Parkinson's diseases.[7] Levodopa (L-DOPA) is used in the treatment of Parkinson's disease and is converted to dopamine by enzymatic reaction (DOPA-decarboxylase).[8] Serotonin (5-HT) is well known to act as a monoamine neurotransmitter in the control and regulation of various brain functions, such as sleep, thermoregulation, food intake, and sexual activity, as well as psychopathological states, such as depression, anxiety, alcoholism, and drug dependency.[9]

Paracetamol or acetaminophen (ACOP), is a long-established and one of the most extensively employed "over the counter" drugs in the world. It is noncarcinogenic and an effective substitute for aspirin for patients with sensitivity to aspirin.[10] However, unlike aspirin, paracetamol's anti-inflammatory activity is considered weak. Nevertheless, it is used to reduce fever, cough and cold, and reduce mild to moderate pain.[11] It is also useful in osteoarthritis therapy,[12] protects hardening of arteries,[13] relieves asthma patients,[14] and protects against ovarian cancer.[15] Therefore, simultaneous detection of neurotransmitters at low concentrations with the presence of ACOP is a challenge of critical importance not only in the field of biomedical chemistry and neurochemistry, but also for diagnostic and pathological research. Simultaneous determination at conventional solid electrodes (carbon or metallic) usually struggles because they undergo overlapping oxidation products.[16] On the other hand, electrochemical methods combines unique characteristics; selectivity, less expensive, and less time-consuming and can potentially be applied to a real-time determination *in vivo*.[17]

Department of Chemistry, Faculty of Science, Cairo University, Post Code 12613 Giza, Egypt. E-mail: nada_fah1@yahoo.com; galalh@sti.sci.eg; Fax: +0235727556; Tel: +0237825266

New materials have recently been extensively used as electrode materials for sensor applications. There are reports of using conducting poly (3-methylthiophene),[18,19] a multiwall carbon nanotubes modified glassy carbon electrode,[20] a carbon paste electrode prepared with 2,2′-[1,2 butanediylbis(nitriloethylidyne)]-bis-hydroquinone and TiO_2 nanoparticles,[21] a nano-TiO_2/polymer coated electrode,[22] a hematoxylin biosensor,[23] palladium nanoclusters-coated polyfuran[24] and a glassy carbon paste electrode modified with polyphenol oxidase.[25]

Nafion® is a cation exchanger that is used for electrode fabrication[26] for the modification of CPE,[37] glassy carbon electrodes,[28] carbon fiber microelectrodes[29] and mercury film electrodes.[30] Nafion films allow the electrolytes to proceed while preventing adsorption:desorption processes of organic species.[31] It is possible to incorporate Nafion into the carbon paste[32] or on top of its surface.[27] Nafion preconcentrates positively charged molecules, which increases the sensitivity of the measurements[33] while retaining ionic selectivity for hydrophobic organic cations.[34]

The carbon paste electrode (CPE), which was made up of carbon particles and organic liquid, has been widely applied in the electroanalytical community due to its low cost, ease of fabrication, high sensitivity for detection and renewable surface.[35] Electrodeposition of gold nanoparticles onto the surface of the CPE was another strategy to enhance the sensitivity of the immunosensor. Several research works have been conducted to construct CPE modified with gold nanoparticles to be used as an immunosensor for the determination of α-fetoprotien,[36] carcinoma antigen,[37] or in streptavidin–biotin interaction,[38] or as enzyme biosensors,[39] also in the determination of hypoxanthine,[40] sulphur containing compounds[41] and homocysteine.[42] Electrodeposition of gold nanoparticles onto other surfaces, such as glassy carbon in sensing of allergen–antibody interaction[43] and acetylcholine esterase–choline oxidase[44] were examined. Monitoring of silver and gold electrodeposition on glassy carbon and silicon,[45] screen-printed[46] and indium/tin oxide surfaces[47] were also studied.

The aim of this study is to construct a novel stable and sensitive electrochemical sensor based on gold nanoparticles, graphite and Nafion®, to be used for the simultaneous determination of ACOP and neurotransmitter compounds in binary mixtures and in the presence of interferences, then compare our results with several other modified electrodes for the assay of ACOP. The electrochemical behaviors of these compounds at the modified electrode will be investigated using CV and differential pulse voltammetry (DPV) techniques. The detection of ACOP in tablet samples and in human urine will be demonstrated as real sample applications.

2. Experimental

2.1. Materials and reagents

Paracetamol (ACOP), dopamine (DA), norepinephrine (NP), epinephrine (EP), levodopa (L-DOPA), serotonin (5-HT), Nafion 10%, ascorbic acid (AA) and uric acid (UA) were purchased from Aldrich and were used as received. Britton–Robinson (B–R) (4.0×10^{-2} M) buffer solution of pH 2–11 ($CH_3COOH + H_3BO_3 + H_3PO_4$), was used as the supporting electrolyte. The pH was adjusted using 0.2 M NaOH. All solutions were prepared from analytical grade chemicals and sterilized Milli-Q deionized water.

2.1.1. Construction of gold nanoparticles modified CPE (CPE–Au_{nano}). CP-electrode was fabricated as described elsewhere[48] then was immersed into 6 mM hydrogen-tetrachloroaurate $HAuCl_4$ solution containing 0.1 M KNO_3 (prepared in doubly distilled water, and deaerated by bubbling with nitrogen). A constant potential of −0.4 V *versus* Ag/AgCl was applied for 400 s. The surface coverage of gold nanoparticles was found to be 2.05×10^{-6} mol cm^{-2}. Then, the modified electrode (CPE–Au_{nano}) was washed with doubly distilled water and dried carefully by a paper without touching the surface and then left to dry in air for ten minutes before being used.

2.1.2. Preparation of gold nanoparticles modified CP/Nafion electrode. The unmodified carbon-paste electrode (CPE) was prepared by mixing graphite powder with appropriate amount of mineral oil (nujol) and thorough hand mixing in a mortar and pestle (75 : 25, w/w, %). A portion of the composite mixture was packed into the end of CPE. To prepare the Nafion-incorporated carbon paste electrode (CPE–Nafion®) [electrode (I)], a mixture of Nafion® solution, nujol and graphite powder (10:15 : 75, w/w, %) with a total weight of 1.00 g was transferred to the mortar and pestle and then homogenized by addition of 2.0 ml of dichloromethane. The solvent was evaporated at room temperature (for 24 h) and the resulting composite was packed in the electrode.[49]

To construct the gold nanoparticles-modified CPE [CPE–Nafion–Au_{nano}, electrode (II)], the electrode was prepared by the same way mentioned to prepare CPE–Nafion followed by electrodeposition of gold nanoparticle.

2.2. Instrumental and experimental set-up

2.2.1. Electrochemical measurements. All voltammetric measurements were performed using a PC-controlled AEW2 electrochemistry work station and data were analyzed with EC_{prog3} electrochemistry software, manufactured by SYCOPEL SCIENTIFIC LIMITED (Tyne & Wear, UK). The one compartment cell with the three electrodes was connected to the electrochemical workstation through a C_3-stand from BAS (USA). A platinum wire from BAS (USA) was employed as the auxiliary electrode. All the cell potentials were measured with respect to Ag/AgCl (3 M NaCl) reference electrode from BAS (USA). One compartment glass cell (15 ml) fitted with gas bubbler was used for electrochemical measurements. Solutions were degassed using pure nitrogen prior and throughout the electrochemical measurements. A JENWAY 3510 pH meter (England) with glass combination electrode was used for pH measurements. Scanning electron microscopy (SEM) measurements were carried out using a JSM-6700F scanning electron microscope (Japan Electro Company). All the electrochemical experiments were performed at an ambient temperature of 25 ± 0.5 °C.

2.2.2. Impedance spectroscopy measurements. Electrochemical impedance spectroscopy was performed using a Gamry-750 system and a lock-in-amplifier that are connected to a personal computer. The data analysis software was provided

with the instrument and applied non-linear least square fitting with the Levenberg–Marquardt algorithm. The parameters in the electrochemical impedance experiment were as follows: different potential values 0.20 V, 0.50 V, applied at a frequency range of 0.1–100 000 Hz with an amplitude of 5 mV, were applied on CPE and CPE–Au_{nano} and tested in ACOP 1.0 mM.

2.3. Analysis of urine

Standard ACOP provided by the National Organization for Drug Control and Research of Egypt was dissolved in urine to make a stock solution with 1.0×10^{-3} M concentration. Successive additions of ACOP 1.0×10^{-3} M in urine were added to 5 ml B–R buffer pH 7.4.

3. Results and discussion

3.1. Morphologies of the different electrodes

The response of the electrochemical sensor was related to its physical morphology. The SEM images of CPE and CPE–Au_{nano} were made,[50] and significant differences in the surface structure of CPE and CPE–Au_{nano} were observed. The surface of the CPE was predominated by isolated and irregularly shaped graphite flakes and separated layers were noticed. On the other hand, the SEM image of CPE–Au_{nano} shows that metallic nanoparticles are located at different elevations over the substrate. Moreover, a random distribution of interstices among the nanoparticles was observed in the SEM image of the CPE–Au_{nano} exhibiting a large surface area.

3.2. Electrochemistry of ACOP and NT compounds at gold nanoparticles modified-CPE (GNMCPE)

The voltammetric behavior of ACOP and some neurotransmitters were examined using cyclic voltammetry. Fig. 1 shows typical cyclic voltammograms of 1.0×10^{-3} M of (A) ACOP, and (B) one of the neurotransmitters (NE), in B–R buffer pH 7.4 at scan rate 100 mV s^{-1} recorded at two different working electrodes (bare CPE (solid line) and CPE–Au_{nano} (dashed lines) electrodes, respectively). As can be seen from Table 1, at CPE–Au_{nano} the oxidation peak current was higher compared to that of bare CPE, whereas the potential shifted negatively to less positive potentials in most cases, due to the improvements in the reversibility of the electron transfer process and a larger apparent surface area of the modified electrode. The electrodeposition of Au particles on the CP-electrode resulted in an observable increase in the peak current, which indicated an improvement in the electrode kinetics and a decrease in the potential of oxidation substantially (*i.e.* thermodynamically feasible reaction). The results confirmed the key role played by Au nanoparticles on the catalytic oxidation, which enhances the electrochemical reaction.

3.3. Effect of operational parameters

3.3.1. Effect of solution pH. The effect of solution pH on the electrocatalytic oxidation of ACOP and the studied neurotransmitters at the CPE–Au_{nano} were studied by cyclic voltammogram using Britton–Robinson buffers within the pH range of 2–11 (figure not shown). It was found that the pH of the solution has a significant influence on the peak potential of the catalytic

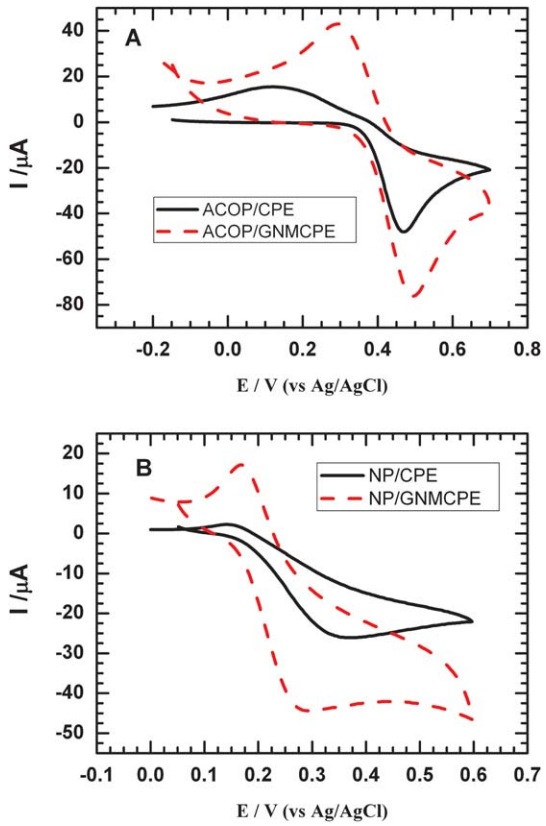

Fig. 1 (A) Cyclic voltammograms of 1.0×10^{-3} M ACOP in B–R buffer pH 7.4 at scan 100 mV s^{-1} recorded at bare CPE (—) and CPE–Au_{nano} (---). (B) Cyclic voltammograms of 1.0×10^{-3} M NP in B–R buffer pH 7.4 at scan rate100 mV s^{-1} recorded at bare CPE (—) and CPE–Au_{nano} (---).

oxidation of ACOP, *i.e.* the anodic peak potentials shifted negatively with the increase of the solution pH, indicating that the electrocatalytic oxidation at the CPE–Au_{nano} is a pH-dependent reaction and that protons have taken part in their electrode reaction processes. Also, the peak potential for ACOP oxidation varies linearly with pH (over the pH range from 2 to 11). The dependence of E_{pa} on pH at the CPE–Au_{nano} can be expressed by the relation:

$$E_{pa}\,(V) = 0.785 - 0.042pH \text{ (}vs.\text{ Ag/AgCl), having correlation coefficient of 0.999.}$$

As paracetamol oxidation is known to involve two protons and two electrons, the slope would be expected to be

Table 1 Comparison between oxidation peak currents and potentials of ACOP and some neurotransmitters

	Bare-CPE		GNMCPE	
Compound	E_{pa} (mV)	I_{pa} (μA)	E_{pa} (mV)	I_{pa} (μA)
Paracetamol	470	48.1	470	65.2
Dopamine	330	20.5	277	35.6
Serotonin	520	20	500	46.2
Norepinephrine	360	11.6	270	31.2
Epinephrine	427	23.2	220	40.3
L-DOPA	400	14.3	340	17.2

59 mV pH^{-1}. The 42 mV pH^{-1} slope obtained in the present studies indicates that the electrode process is more complex.

The current response was also affected by changing the pH of the medium, thus, Fig. 2 shows the graph of current response of some neurotransmitters and ACOP, at different pH values, at (A) bare CPE and (B) CPE–Au_{nano}, respectively. It is clear that at CPE–Au_{nano} the anodic current responses for all neurotransmitters and ACOP, at the whole pH range are higher than that at bare CPE. Using CPE–Au_{nano}, it was found that all neurotransmitters and ACOP gave their highest anodic current responses at low pH values, while at higher pH values the response was lower, and there are high responses at a wide variety of pH values. Because the pK_a values are 9.5 for ACOP,[51] 8.9 and 10.6 for DA,[52] 8.55 for EP,[53] 8.4 for NE,[54] 9.97 and 10.73 for 5-HT;[55] therefore, they all carry positive charge at pH values lower than their pK_a values. This should result in attraction forces between these positive charges and the gold nanoparticles' negative charge, which indicates the effect of gold nanoparticles on the catalytic oxidation processes, except for L-DOPA, with pK_a 2.31, 8.71, 9.74 and 13.4, it is neutral at pH 7.4[56] so the current response does not increase as much as the other compounds.

3.3.2. Stability of the response of the modified electrode. In order to investigate the response stability of CPE–Au_{nano}, the CV for 1.0×10^{-3} M ACOP in B–R buffer (pH 7.4) solution were recorded every five minutes and it stands for fifty runs (Fig. 3). It was found that the anodic and cathodic peak currents remained practically the same. Repetitive measurements indicated that this electrode has good reproducibility and does not undergo surface fouling during the voltammetric measurements.

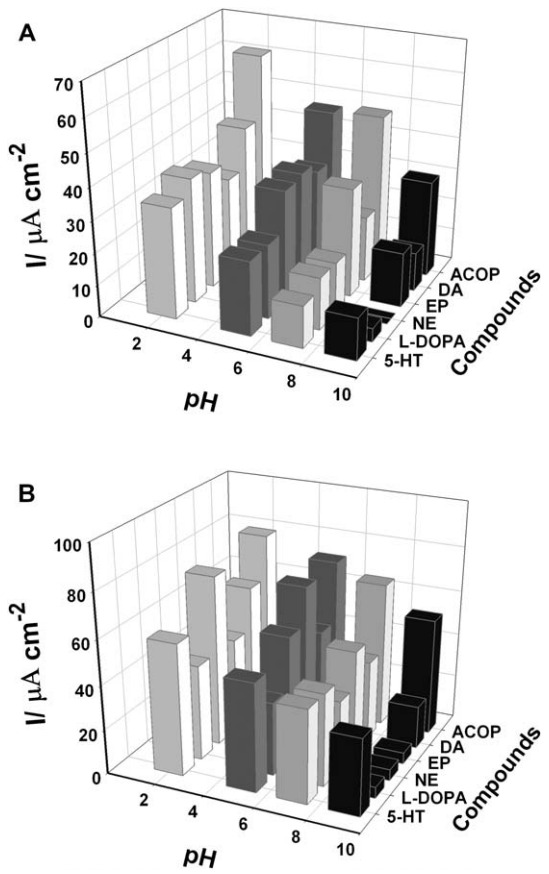

Fig. 2 (A) A graph of current response of some neurotransmitters and ACOP, at different pH values, at the bare CP-electrode. (B) A graph of current response of some neurotransmitters and ACOP, at different pH values, at CPE–Au_{nano}.

3.3.3. Influence of the scan rate. The effect of different scan rates (ν ranging from 10 to 250 mV s^{-1}) on the current response of ACOP (1.0×10^{-3} M) on CPE–Au_{nano} in B–R buffer (pH 7.4) was studied and a plot of peak current (i_p) *versus* the square root of the scan rate ($\nu^{1/2}$) gave a straight line relationship. This revealed that the linearity of the relationship was realized up to a scan rate of 250 mV s^{-1}. This indicated that the charge transfer was under diffusion control. Typical CV curves of ACOP at different scan rates are shown in Fig. 4. The peak-to-peak separation also increased with increasing the scan rate. A good linear relationship was found for the oxidation and the reduction peak currents, with different scan rates (Fig. 4 inset). The reduction and oxidation peak currents increased linearly with the linear regression equations as:

$$i_{pa}\ (10^{-6}\ A) = -2.037\nu^{1/2}\ (V\ s^{-1})^{1/2} - 7.160\ (n = 7,\ \gamma = 0.9965),$$

$$i_{pc}\ (10^{-6}\ A) = 3.461\nu^{1/2}\ (V\ s^{-1})^{1/2} - 5.296\ (n = 7,\ \gamma = 0.9899),$$

respectively.

This suggests that the reaction is diffusion-controlled electrode reaction.

3.3.4. Diffusion coefficients of ACOP and NT compounds. The dependence of the anodic peak current density on the scan rate has been used for the estimation of the "apparent" diffusion coefficient, D_{app}, for the compounds studied. D_{app} values were calculated from the Randles Sevcik equation,[57] and for the oxidized species [O]:

$$I_p = 0.4463(F^3/RT)^{1/2}n^{3/2}\upsilon^{1/2}D_0^{1/2}AC_0$$

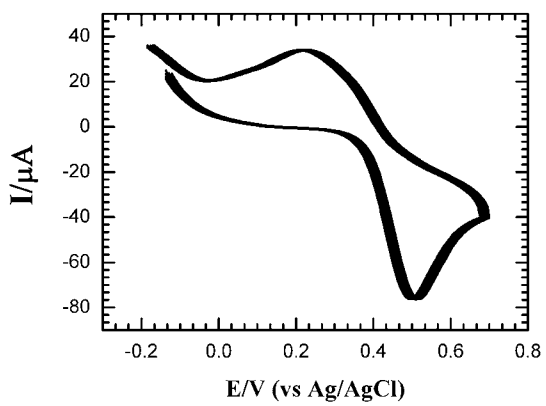

Fig. 3 Cyclic voltammograms (CV) for 1.0×10^{-3} M ACOP in B–R buffer (pH 7.4) solution recorded every five minutes for fifty runs.

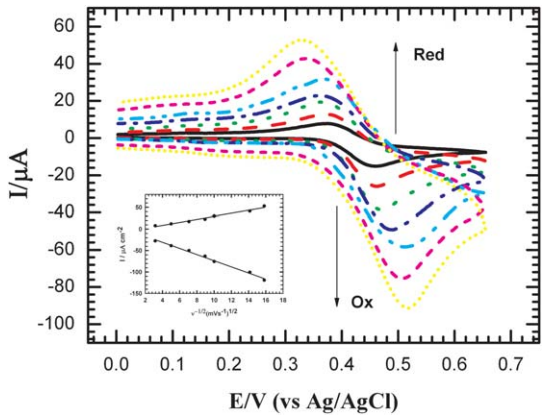

Fig. 4 Cyclic voltammograms (CV) of 1.0×10^{-3} M ACOP at the CPE–Au_{nano} in 0.04 M B–R buffer pH 7.4 at: 10, 25, 50, 80, 100, 200 and 250 mV s^{-1}.The inset: plot of the anodic and cathodic peak current values *versus* square root of scan rate.

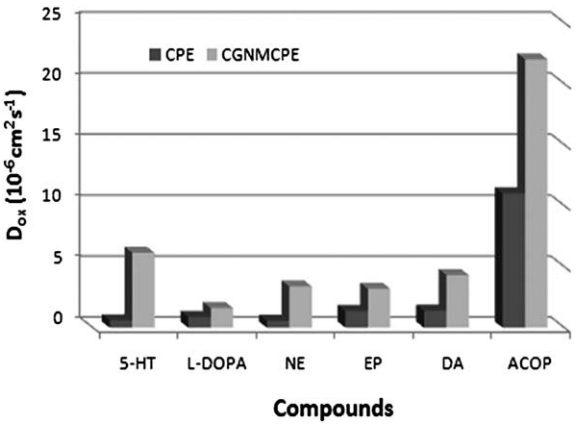

Fig. 5 A graph indicating the apparent diffusion coefficients, D_{app}, of ACOP and the studied neurotransmitters on GNMCPE and bare CP electrode.

For $T = 298$ K (at which temperature the experiments were conducted), the equality holds true:

$$I_{pa} = (2.69 \times 10^5) n^{3/2} A C_0^* D_0^{1/2} v^{1/2}$$

Where the constant has the units: 2.687×10^5 C mol^{-1} $V^{-1/2}$.

In these equations: I_p is the peak current density (A cm^{-2}), n is the number of electrons appearing in the half-reaction for the redox couple, v is the rate at which the potential is swept (V s^{-1}), F is Faraday's constant (96 485 C mol^{-1}), C_0 is the analyte concentration (1×10^{-6} mol cm^{-3}), A is the electrode area (0.0706 cm^2), R is the universal gas constant (8.314 J mol^{-1} K^{-1}), T is the absolute T/K, and D is the electroactive species diffusion coefficient (cm^2 s^{-1}). Apparent surface area used in the calculations did not take into account the surface roughness.

The apparent diffusion coefficients, D_{app}, of ACOP and the studied neurotransmitters on CPE–Au_{nano} E in B–R buffer (pH 7.4) were calculated from cyclic voltammetry (CV) experiments and were in the range of (1.0×10^{-6}–2.2×10^{-5} cm^2 s^{-1}), these results were compared to those calculated in the case of bare CPE, which were in the range of (5.94×10^{-7}–1.1×10^{-5} cm^2 s^{-1}), as shown in Fig. 5. This graph indicated the quick mass transfer of the analyte molecules towards the CPE–Au_{nano} surface from bulk solutions and/or fast electron transfer process of electrochemical oxidation of the analyte molecule at the electrode-solution interface.[58,59] Furthermore, it also showed that the redox reaction of the analyte species took place at the surface of the electrode under the control of the diffusion of the molecules from solution to the electrode surface. The calculated D_{app} values at the bare CPE and CPE–Au_{nano} showed that Au nanoparticles improve the electron transfer kinetics at the electrode/solution interface.

3.4. Electrochemical impedance spectroscopy (EIS) studies

EIS is an effective tool for studying the interface properties of surface-modified electrodes. EIS data were obtained for GNMCPE at ac frequency varying between 0.1 Hz and 100 kHz with an applied potential in the region corresponding to the electrolytic oxidation of ACOP in B–R buffer pH 7.4. Fig. 6 shows a typical impedance spectrum presented in the form of Nyquist plot of ACOP using GNMCPE at the oxidation (A) and the reduction (B) potentials, the insets represents the Nyquist plot of ACOP using the bare CP-electrode. From this comparison, it is clear that the impedance responses of ACOP show a great difference in the presence of gold nanoparticles.

The semicircle diameter in the impedance spectrum equals the electron-transfer resistance, R_{et}. This resistance controls the electron-transfer kinetics of the redox probe at the electrode interface. Therefore, R_{et} can be used to describe the interface properties of the electrode. To obtain detailed information from the impedance spectroscopy, a simple equivalent circuit model in Fig. 6C was used to fit the results.

The experimental data were compared to an "equivalent circuit". In this circuit, R_u is the solution resistance, R_p is the polarization resistance and CPhE represents the predominant diffusion influence on the ionic/electronic charge transfer process, n is its corresponding exponents. C_f is the capacitance of the double layer and W is the Warburg impedance due to diffusion Table 2 lists the best fitting values calculated from the equivalent circuit for the impedance data. From the data indicated in Table 2, the value of solution resistance, R_u, was almost constant within the limits of the experimental errors. The average error (χ^2) of the fits for the mean error of modulus was in the range of $\chi^2 = (1.0–2.3) \times 10^{-2}$. On the other hand, the ionic/electronic charge transfer resistance, CPhE, shows noticeable decrease in values in case of CPE–Au_{nano} *versus* CPE, which indicates less electronic resistance and more facilitation of charge transfer. The capacitive component of the charge at the CPE–Au_{nano} is relatively higher compared to that at the CPE. This is explained in terms of the increase in the ionic adsorption at the electrode/electrolyte interface. Moreover, the decrease in the interfacial electron transfer resistance is attributed to the selective interaction between gold nanoparticles and ACOP that resulted in the observed increase in the current signal for the electro-oxidation process.

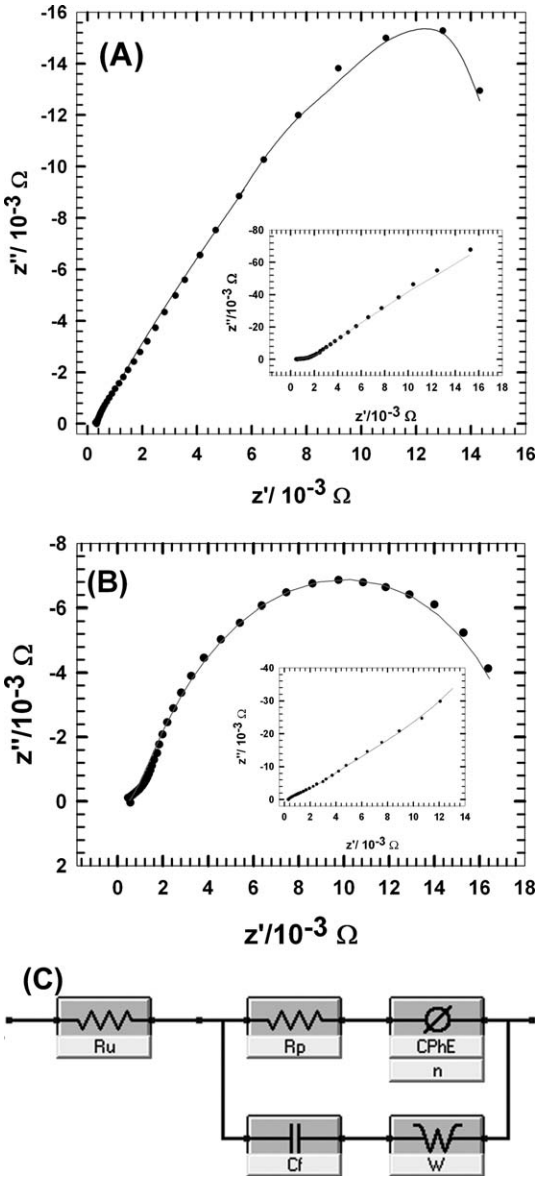

Fig. 6 (A) The typical impedance spectrum presented in the form of the Nyquist plot for ACOP using CPE–Au_{nano} at the oxidation potential 500 mV. The insets represent the Nyquist plot of ACOP using the bare CP-electrode. (Symbols and solid lines represent the experimental measurements and the computer fitting of impedance spectra, respectively). (B) The typical impedance spectrum presented in the form of the Nyquist plot for ACOP using CPE–Au_{nano} at the reduction potential 200 mV. The insets represent the Nyquist plot of ACOP using the bare CPE. (Symbols and solid lines represent the experimental measurements and the computer fitting of impedance spectra, respectively). (C) The equivalent circuit used in the fit procedure of the impedance spectra.

3.5. The effect of Nafion® for improvement of the electrocatalytic effect of ACOP

To illustrate the effect of Nafion® with gold nanoparticles, ACOP was examined using cyclic voltammetry. Fig. 7 shows typical cyclic voltammograms of 1.0×10^{-3} M of (A) ACOP in B–R buffer pH 7.4 at scan rate 100 mV s^{-1} at [electrode (I), CPE–Nafion®] (solid line) and [electrode (II), CPE–Nafion®–Au_{nano}]. As can be seen, at [electrode (II)] the oxidation peak current was 112.1 μA, which was higher compared to that of [electrode (I)], which was 45.2 μA, this is due to the larger surface area of the modified electrode and the synergism effect of the electronic conductivity and electroactivity of gold metallic properties with ionic conductivity and the ion-exchange capacity of Nafion®, furthermore, the accumulation mechanism of Nafion®, which can be explained through an electrostatic interaction between the film and ACOP due to the hydrophilic negatively charged sulfonate groups of Nafion® in the polymer structure, which causes an improvement in the reversibility of the electron transfer process and enhancement in the electrochemical reaction of ACOP. The electrochemical oxidation of paracetamol is followed by chemical steps, the pathways of which are dependent on both pH and the voltammetric scan rate.[60,61]

3.6. Effect of interferences on the behavior of ACOP

In biological samples, AA and UA are the common important interferences for the determination of neurotransmitters at sensor surfaces. To check the sensitivity and selectivity of the

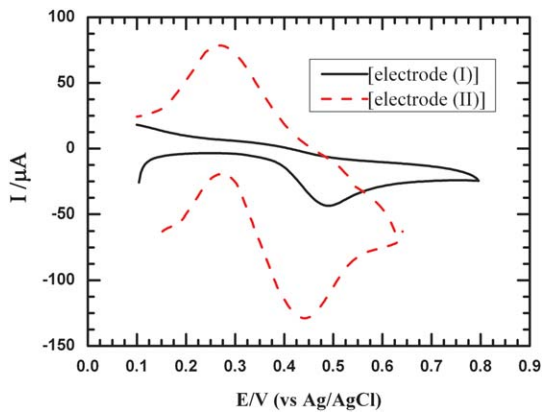

Fig. 7 Cyclic voltammograms of 1.0×10^{-3} M of (A) ACOP in B–R buffer pH 7.4 at scan rate 100 mV s^{-1} at [electrode (I)] (solid line) and [electrode (II)].

Table 2 Electrochemical impedance spectroscopy fitting data corresponding to Fig. 9 (A and B)

Electrode	E (mV)	R_p (kΩ cm^2)	R_u (kΩ cm^2)	C_f (μFcm^{-2})	W (kΩ^{-1}cm^{-2})	CPhE (μFcm^{-2})	n
Bare CPE	200	1000	0.51	5.71	28.33	34.73	0.61
	500	950	0.51	5.78	28.71	52.95	0.80
CPE–Au_{nano}	200	85.5	0.51	39.63	9.92	57.09	0.72
	500	37.0	0.52	49.16	5.52	85.59	0.64

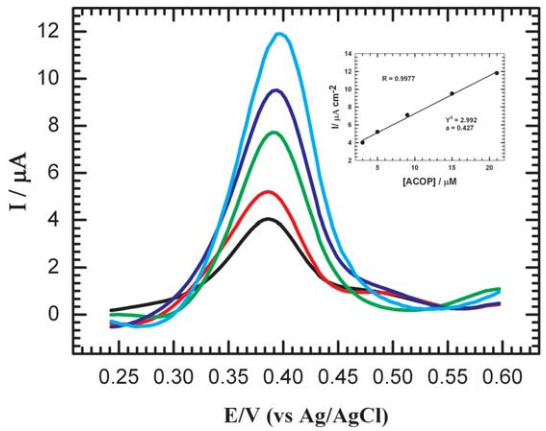

Fig. 8 Voltammetric current responses of successive additions of ACOP using [electrode (II)] in B–R buffer (pH 7.4), containing 1.0 mM AA and 1.0 mM UA.

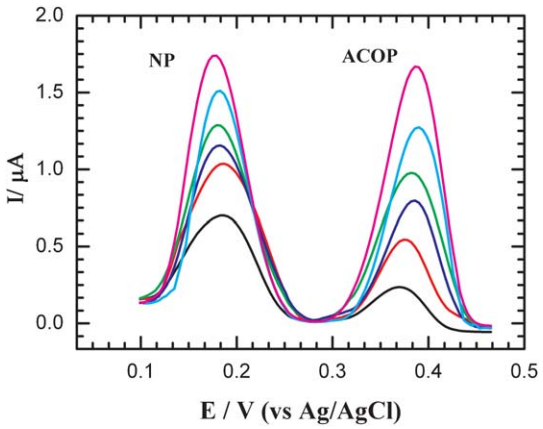

Fig. 9 Differential pulse voltammograms (DPVs) obtained for a ACOP and NP mixture on [electrode (II)] in B–R buffer (pH 7.4) by changing the concentration of both ACOP and NP.

sensor in the presence of these interferences, the voltammetric current responses of successive additions of ACOP were recorded Fig. 8, using [electrode (II)] in B-R buffer (pH 7.4), containing 1.0 mM AA and 1.0 mM UA. The inset of Fig. 8 shows the calibration plot of ACOP in the presence of the interfering substance, it was observed that there was no change in the peak currents or limit of detection for ACOP under the potential range used. So AA and UA did not interfere with ACOP at [electrode (II)]. This behavior could be explained on the basis of the negatively charged surface of the [electrode (II)] in its anionic form at the working pH of 7.4, ACOP with a pK_a of 9.5 was mainly in its cationic form, which can be attracted to the electrode surface, while AA with a pK_a of 4.2[62] and UA with a pK_a of 5.4[62] were in their anionic forms, which were repelled by the negatively charged gold particles.[63] Also AA and UA remain negatively charged due to resonance stability of their structure and they can easily donate a proton in the medium of pH 7.4, consequently they do not interfere with ACOP. From the above results we can conclude that [electrode (II)] can be applied successfully for the determination of ACOP in the presence of AA and UA.

3.7. Simultaneous determination of ACOP and the studied NT compounds

Simultaneous determinations of ACOP with different neurotransmitters of low concentration in binary mixtures were studied using [electrode (II)]. Fig. 9 shows the differential pulse voltammograms (DPVs) obtained for a ACOP and NP mixture at [electrode (II)] in B–R buffer (pH 7.4) by changing the concentration of both ACOP and NP. The oxidation peaks of NP (at 180 mV) and ACOP (at 0.39 V) with a peak separation of 210 mV were observed. With increasing the concentrations of both compounds, the current responses of both ACOP and NP linearly increased with a correlation coefficient of 0.997 and 0.992, respectively, also the regression equation for ACOP was found to be:

$$I_p\ (\mu A) = 0.04c\ (\mu M) - 0.031,$$

The regression equation for NP was:

$$I_p\ (\mu A) = 0.045c\ (\mu M) + 0.7052.$$

3.8. Analytical characterization of ACOP and its reproducibility

Pulse voltammetric techniques, such as DPV, are effective and rapid electroanalytical techniques with well-established advantages, including good discrimination against background current and low detection limits. To prove the sensitivity of [electrode (II)] towards the electrochemical measurement of ACOP, the effect of changing the concentration of ACOP in B–R buffer pH 7.4, using DPV mode was studied (Fig. 10). The following are the parameters for the DPV experiments: E_i = 0.0 mV, E_f = +600 mV, scan rate = 10 mV s^{-1}, pulse width = 25 ms, pulse period = 200 ms, and pulse amplitude = 10 mV. The

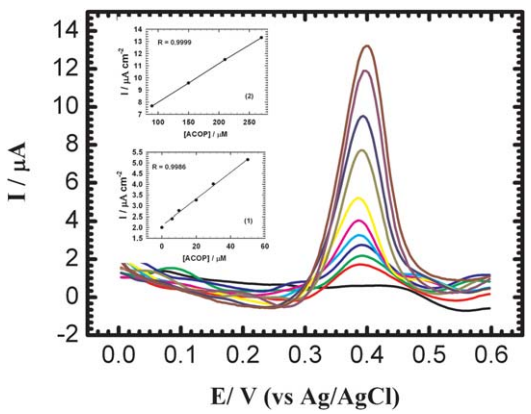

Fig. 10 The effect of changing the concentration of ACOP, using differential pulse mode at CPE–Au_{nano} in 0.04 M B–R buffer pH 7.4 and scan rate 10 mV s^{-1}. The inset (1): represents the differential pulse mode of the smaller concentration range. The inset (2): represents the differential pulse mode of the larger concentration range.

Table 3 Comparison of the CPE–Au_{nano} with the reported methods for the determination of (ACOP)

Sample No.	Ref. No.	Electrode used	Limit of Detection (LOD)
1	64	Dipyrromethene-Cu(II) monolayers modified gold electrode	1.2×10^{-4} M
2	65	Carbon ionic liquid electrode	0.3×10^{-6} M
3	66	Nanogold modified indium tin oxide electrode	1.8×10^{-7} M
4	67	Fullerene modified glassy carbon electrode	5.0×10^{-5} M
5	68	Boron-doped diamond electrode	4.9×10^{-7} M
6	69	MWNT modified basal plane pyrolytic graphite electrode	1.0×10^{-8} M
7	70	CNT modified screen-printed carbon electrode	1.0×10^{-7} M
8	This work	AuNps modified Nafion/CP electrode	7.7×10^{-9} M

Table 4 Recovery data obtained by the standard addition method for (ACOP) in drug formulation

Formulation	[tablet] taken $\times 10^{-6}$/M	[standard] added $\times 10^{-6}$/M	Found(M) $\times 10^{-6}$/M	Recovery (%)	RSD (%)
Paracetamol	6.0	2.0	7.99	99.8	1.22
	20.0	—	22.28	101.2	1.39
	50.0	—	52.09	100.1	0.24
	210.0	—	211.88	99.9	0.09

Table 5 Evaluation of the accuracy and precision of the proposed method for the determination of ACOP in urine samples

[ACOP] added (M) $\times 10^{-6}$	[ACOP] Found[a](M) $\times 10^{-6}$	Recovery (%)	SD $\times 10^{-7}$	S.E[b] $\times 10^{-7}$	C.L.[c] $\times 10^{-7}$
0.6	0.612	102.0	0.23	0.10	0.29
2.0	2.024	101.2	0.51	0.23	0.63
10.0	10.10	101.0	2.64	1.18	3.28
50.0	49.80	99.6	2.09	0.85	2.20

[a] mean for five determinations. [b] Standard error = SD/$\sqrt{n}$. [c] C.L. confidence at 95% confidence level and 4 degrees of freedom ($t = 2.776$).

corresponding calibration plots are given in the insets. The calibration plot was linearly related to ACOP concentration over the ranges of 5.0×10^{-8}–5.0×10^{-5} M with the regression equation of I_p (μA) = 0.0619c (μM) + 2.08, and 9.0×10^{-5}–2.7×10^{-4} mol L^{-1} with the regression equation of I_p (μA) = 0.0314c (μM) + 7.86 and the correlation coefficients are 0.999 and 0.999, respectively. The limits of detection (LOD) and the limits of quantitation (LOQ) were calculated from the oxidation peak currents of the two linear ranges using the following equations: LOD = 3s/m, LOQ = 10s/m, where s is the standard deviation of the oxidation peak current (three runs) and m is the slope (μA M^{-1}) of the related calibration curves, and they were found to be 7.7×10^{-9} M and 2.5×10^{-8} M, respectively for the first linear range, and 2.8×10^{-8} M and 9.5×10^{-8} M, respectively, for the second linear range. Both LOD and LOQ values confirmed the sensitivity of [electrode (II)].

Table 3 shows a comparison of the LOD of [electrode (II)] with the reported methods for the determination of paracetamol. Our work showed the lowest limit of detection compared to the other values mentioned in the literature using other modified electrodes.

3.9. Validation in pharmaceutical samples

Commercial pharmaceutical samples (tablets) containing paracetamol was analyzed to evaluate the validity of the proposed method. Paracetamol tablets containing 500 mg ACOP were applied from SEDICO Pharmaceutical Company (Egypt). The tablets were weighed and finely pulverized. The appropriate amount of this powder was dissolved in double distilled water. The content of the tablet was diluted to obtain the concentration of paracetamol in the working range and then DPV were recorded using [electrode (II)]. The concentration of paracetamol in the pharmaceutical formulations was determined from the calibration curve. Average concentrations were calculated from five replicate measurements of two independent solutions of the same pharmaceutical preparations. Table 4 shows the data generated by standard addition method for the analysis of paracetamol in buffered solution of pH 7.4. The data shows that the content values determined by the proposed method for the commercial samples are very close to the claimed amount. The analysis of the obtained responses allowed the conclusion that the drug excipients do not significantly interfere with the proposed method. Thus, the practical application was demonstrated with the determination of paracetamol directly in pharmaceutical formulations with satisfactory results. From Table 4 we can see that the recovery data obtained by the standard addition method for ACOP in drug formulations was found in the range from 99.8% to 101.2% and the relative standard deviation (RSD) was in the range from 0.09% to 1.39%, suggesting that [electrode (II)] has a high reproducibility and it would be a useful electrode for the quantitative analysis of ACOP in pharmaceutical formulations.

3.10. Validation of the method in real samples of urine

Validation of the procedure for the quantitative assay of the ACOP was examined in B–R buffer pH 7.4, at a scan rate of

10 mV s^{-1} using DPV. The calibration curve gave a straight line in the linear dynamic range 6×10^{-7}–1.9×10^{-4} M with correlation coefficient, $R = 0.999$, the LOD is 1.6×10^{-8} M. Four different concentrations on the calibration curve are chosen to be repeated five times to evaluate the accuracy and precision of the proposed method, which is represented in Table 5. The use of Nafion® improved the performance of the sensor and resulted in better resolution and LOD.[71,72]

4. Conclusion

In the present work, a sensor based on a CP-electrode modified with gold nanoparticles was used for the electrochemical determination of ACOP and some neurotransmitters. Gold nanoparticles enhanced the sensitivity of CPE towards different compounds; furthermore, gold nanoparticles Nafion® carbon paste modified electrode has been proved to be efficient for the electrocatalytic oxidation of paracetamol in biological fluids.

Simultaneous determinations of ACOP with NP in a binary mixture were achieved with good separation. On the other hand, selective determination of ACOP with high current response is obtained in presence of AA and UA, and the method was simple, sensitive and successfully applied for determination of ACOP in human urine and in commercial tablets with good precision and accuracy. The LOD range is 10^{-8}–10^{-9} in standard and real samples, respectively, within the confidence error.

5. Acknowledgment

The authors would like to express their gratitude to the University of Cairo (Office of Vice President for Graduate Studies and Research) for providing partial financial support through "The Young Researchers' Program." We would like to acknowledge the financial support by the National Organization for Drug Control and Research (NODCAR, Egypt).

References

1 Z. D. Sandlin, M. S. Shou, J. G. Shackman and R. T. Kennedy, *Anal. Chem.*, 2005, **77**, 7702.
2 M. Ebadi, S. Sharma, S. Shavali and H. E. L. Refaey, Neuroprotective actions of selegiline, *J. Neurosci. Res.*, 2002, **67**, 285–289.
3 C. Bruhlmann, F. Ooms, P. A. Carrupt, B. Testa, M. Catto, F. Leonetti, C. Altomare and A. Carotti, *J. Med. Chem.*, 2001, **44**, 3195.
4 A. J. Shah, F. Crespib and C. Heidbrederb, *J. Chromatogr., B: Anal. Technol. Biomed. Life Sci.*, 2002, **781**, 151.
5 S. K. Lunsford, H. Choi, J. Stinson, A. Yeary and D. D. Dionysiou, *Talanta*, 2007, **73**, 172.
6 R. M. Carney, K. E. Freedland, R. C. Veith, P. E. Cryer, J. A. Skala, T. Lynch and A. S. Jaffe, *Biol. Psychiatry*, 1999, **45**, 458.
7 K. S. Rommelfanger and D. Weinshenker, *Biochem. Pharmacol.*, 2007, **74**, 177.
8 W. J. Weiner, *Diagnosis & Clinical Management*, Demos Medical Publishing, New York, ISBN: 1-888799-50-1, 2002, p 195.
9 K. H. Le Quan-Bui, O. Plaisant and M. Leboyer, *Psychiatry Res.*, 1984, **13**, 129.
10 *Martindale the Extra Pharmacopoeia*, ed. A. Wade, 27th edn, The Pharmaceutical Press, London, 1979.
11 C. J. Nikles, M. Yelland, C. D. Marc and D. Wilkinson, *Am. J. Ther.*, 2005, **12**, 80.
12 K. Brandt, *Drugs*, 2003, **63**, 23.
13 A. A. Taylor, *Baylor College of Medicine-Abstract from Munich Meeting (Thirteenth IUPHAR Congress of Pharmacology)*, 1998.
14 National Asthma Campaign; Fact sheet 09, http://blog.asthma.org.uk/wheezing_is_not_the.html, 2009.
15 D. W. Cramer, B. L. Harlow, L. T. Ernstoff, K. Bohlke, W. R. Welch and E. R. Greenberg, *Lancet*, 1998, **351**, 104.
16 H. R. Zare, N. Nasirizadeh and M. M. Ardakani, *J. Electroanal. Chem.*, 2005, **577**, 25.
17 Z. Gao, K. S. Siow, A. Ng and Y. Zhang, *Anal. Chim. Acta*, 1997, **343**, 49.
18 N. F. Atta and M. F. El-Kady, *Talanta*, 2009, **79**, 639.
19 N. F. Atta, A. Galal, A. E. Karagözler, G. C. Russell, H. Zimmer and Harry B. Mark, Jr., *Biosens. Bioelectron.*, 1991, **6**, 333.
20 Z. A. Alothman, N. Bukhari, S. M. Wabaidur and S. Haider, *Sens. Actuators, B*, 2010, **146**, 314.
21 M. M. Ardakani, H. Beitollahi, M. A. Sheikh Mohseni, A. Benvidi, H. Naeimi, M. Nejati-Barzoki and N. Taghavinia, *Colloids Surf., B*, 2010, **76**, 82.
22 S. Ashok Kumar, C. F. Tang and S. M. Chen, *Talanta*, 2008, **76**, 997.
23 N. Nasirizadeh and H. R. Zare, *Talanta*, 2009, **80**, 656.
24 N. F. Atta, M. F. El-Kady and A. Galal, *Sens. Actuators, B*, 2009, **141**, 566.
25 M. C. Rodríguez and G. A. Rivas, *Anal. Chim. Acta*, 2002, **459**, 43.
26 C. P. Andrieux, P. Audebert, B. Divisia-Blohorn, P. Aldebert and F. Michalak, *J. Electroanal. Chem.*, 1990, **296**, 117.
27 S. Moane, J. R. Barreira, M. Ordieres, P. Tunon and M. R. Smyth, *J. Pharm. Biomed. Anal.*, 1995, **14**, 57.
28 H. Li, Y. Li, J. Li, E. Wang and S. Dong, *Electroanalysis*, 1995, **7**, 742.
29 J. Weber, L. Dunsch and A. Neudeck, *Electroanalysis*, 1995, **7**, 255.
30 S. Capelo, A. M. Mota and M. L. S. Goncalves, *Electroanalysis*, 1995, **7**, 563.
31 H. Li, R. Ge and E. Wang, *Anal. Chim. Acta*, 1994, **292**, 107.
32 D. Boyd, J. R. Barreira Rodriguez, P. Tunon Blanco and M. R. Smyth, *J. Pharm. Biomed. Anal.*, 1994, **12**, 1069.
33 C. R. Martin and H. Freiser, *Anal. Chem.*, 1981, **53**, 902.
34 J. Zhou and E. Wang, *Anal. Chim. Acta*, 1991, **249**, 489.
35 N. S. Lawrence, R. P. Deo and J. Wang, *Anal. Chem.*, 2004, **76**, 3735.
36 C. Ding, F. Zhao, R. Ren and J. M. Lin, *Talanta*, 2009, **78**, 1148.
37 D. Tang, R. Yuan and Y. Chai, *Anal. Chim. Acta*, 2006, **564**, 158.
38 M. B. González-García, C. Fernández-Sánchez and A. Costa-García, *Biosens. Bioelectron.*, 2000, **15**, 315.
39 M. L. Mena, P. Yáñez-Sedeño and J. M. Pingarrón, *Anal. Biochem.*, 2005, **336**, 20.
40 L. Agüí, J. Manso, P. Yáñez-Sedeño and J. M. Pingarrón, *Sens. Actuators, B*, 2006, **113**, 272.
41 L. Agüí, J. Manso, P. Yáñez-Sedeño and J. M. Pingarrón, *Talanta*, 2004, **64**, 1041.
42 L. Agüí, C. Peña-Farfal, P. Yáñez-Sedeño and J. M. Pingarrón, *Talanta*, 2007, **74**, 412.
43 H. Huang, P. Ran and Z. Liu, *Bioelectrochemistry*, 2007, **70**, 257.
44 S. Upadhyay, G. R. Rao, M. K. Sharma, B. K. Bhattacharya, V. K. Rao and R. Vijayaraghavan, *Biosens. Bioelectron.*, 2009, **25**, 832.
45 K. Márquez, R. Ortiz, J. W. Schultze, O. P. Márquez, J. Márquez and G. Staikov, *Electrochim. Acta*, 2003, **48**, 711.
46 M. Moreno, E. Rincon, J. M. Pérez, V. M. González, A. Domingo and E. Dominguez, *Biosens. Bioelectron.*, 2009, **25**, 778.
47 Y. Ma, J. Di, Xi, X. Yan, M. Zhao, Z. Lu and Y. Tu, *Biosens. Bioelectron.*, 2009, **24**, 1480.
48 J. Zheng and X. Zhou, *Bioelectrochemistry*, 2007, **70**, 408.
49 S. Shahrokhian and M. Ghalkhani, *Electrochim. Acta*, 2006, **51**, 2599.
50 N. F. Atta, A. Galal, F. M. Abu-Attia and S. M. Azab, *J. Electrochem. Soc.*, 2010, **157**, 116.
51 X. Jiang and X. Lin, *Anal. Chim. Acta*, 2005, **537**, 145.
52 A. C. Moffat, in *Clarcke's Isolation and Identification of Drugs*, The Pharmaceutical Press, London, 1986, pp. 520, 849, 944.
53 *Handbook of Chemistry and Physics*, ed. D. R. Lide, 84th edition, CRC Press, 2004.
54 P. Y. Bruice, *Organic Chemistry*, 5th edn, Person Prentice-Hall, New Jersey, 2007, p. 314.
55 P. N. Palma, M. L. Rodrigues, M. Archer, M. J. Bonifacio, A. I. Loureiro, D. A. Learmonth, M. A. Carrondo and P. Soares-da-Silva, *Mol. Pharmacol.*, 2006, **70**, 143.
56 J. Pratuangdejkul, W. Nosoongnoen, G. A. Urin, S. Loric, M. Conti, J. M. Launay and P. Manivet, *Chem. Phys. Lett.*, 2006, **420**, 538.
57 N. F. Atta, A. Galal and R. A. Ahmed, *Bioelectrochemistry*, 2011, **80**, 132.

58 N. Yang, Q. Wan and J. Yu, *Sens. Actuators, B*, 2005, **110**, 246.
59 W. Qijin, Y. Nianjun, Z. Haili, Z. Xinpin and X. Bin, *Talanta*, 2001, **55**, 459.
60 J. Y. Lewis, W. R. Heineman, D. A. Roston and P. T. Kissinger, *J. Chem. Educ.*, 1983, **60**, 772.
61 D. J. Miner, J. R. Rice, R. M. Riggin and P. T. Kissinger, *Anal. Chem.*, 1981, **53**, 2258.
62 V. S. Vasantha and S.-M. Chen, *J. Electroanal. Chem.*, 2006, **592**, 77.
63 J. Li and X.-Q. Lin, *Anal. Chim. Acta*, 2007, **596**, 222.
64 B. Saraswathyamma, I. Grzybowska, C. Orlewska, J. Radecki, W. Dehaen, K. G. Kumar and H. Radecka, *Electroanalysis*, 2008, **20**, 2317.
65 X. ShangGuang and H. Zhang, *Anal. Bioanal. Chem.*, 2008, **391**, 1049.
66 R. N. Goyal, V. K. gupta, M. Oyama and N. Bachheti, *Electrochem. Commun.*, 2005, **7**, 803.
67 R. N. Goyal and S. P. Singh, *Electrochim. Acta*, 2006, **51**, 3008.
68 B. C. Lourenção, R. A. Medeiros, R. C. Rocha-Filho, L. H. Mazo and O. Fatibello-Filho, *Talanta*, 2009, **78**, 748.
69 R. T. Kachoosangi, G. G. Widgoose and R. G. Compton, *Anal. Chim. Acta*, 2008, **618**, 54.
70 P. Fanjul-Bolado, P. J. Lamas-Ardisana, D. Hernández-Santos and A. Costa-García, *Anal. Chim. Acta*, 2009, **638**, 133.
71 J.-H. Jung, J.-H. Jeon, V. Sridhar and I.-K. Oh, *Carbon*, 2011, **49**, 1279.
72 C. Li, E. T. Thostenson and T.-W. Chou, *Compos. Sci. Technol.*, 2008, **68**, 1227.

